Supporting Information

Characterization of Arylalkylamine *N*-Acyltransferase from *Tribolium castaneum*: An Investigation into a Potential Next-Generation Insecticide Target

Brian G. O'Flynn[†], Eric M. Lewandowski[‡], Karin Claire Prins[†], Gabriela Suarez[†], Angelica N. McCaskey[†], Nasha M. Rios-Guzman[†], Ryan L. Anderson[†,‖], Britney A. Shepherd[†], Ioannis Gelis[†], James W. Leahy[†,‡,§], Yu Chen[‡], & David J. Merkler*[†]

† Department of Chemistry, University of South Florida, Tampa, Florida, 33620, United States

‡ Department of Molecular Medicine, University of South Florida College of Medicine, Tampa, 33612, United States

§ Center for Drug Discovery and Innovation, University of South Florida, Tampa, Florida, 33620, United States

‖ Department of Biochemistry and Molecular Genetics, University of Colorado Anschutz Medical Campus, Aurora, CO 80238.

Cloning of *T. castaneum* AANAT0.

The codon-optimized gene for *T. castaneum* AANAT0 (NCBI accession number: XM_967780.4) was synthesized by Genscript and ligated into a *pET-28a* vector using *XhoI and NdeI* restriction sites. The vector was transformed into XL-10 *E. coli* competent cells for vector consolidation and, subsequently, into *E. coli* BL21 (DE3) for protein expression. The cells containing the *TcAANAT0-pET-28a* vectors were cultured in 20 g/L LB media, supplemented with 50 μg/mL kanamycin at 37°C until an optimal OD_{600} ~ 0.6 was reached. 1.0 mM isopropyl β-D-1-thiogalactopyranoside (IPTG) was added to induce transcription and the batches were left to culture for a further 4 hours. The culture was centrifuged at 5000 × g for 10 min at 4 °C and the resulting pellet resuspended in a buffer of 20 mM Tris, pH 8.0, 500 mM NaCl, and 5 mM imidazole. The cells were lysed via sonication and the lysate centrifuged at 10,000 × g for 20 min at 4°C. The supernatant containing the protein of interest, decorated with an N-terminal His_6-tag, was collected and loaded onto 6 mL of HisPur nickel-nitrilotriacetic acid (Ni-NTA) chelating resin for purification via affinity chromatography. The resin was charged with 10 column volumes (CVs) of 20 mM Tris, pH 8.0, 500 mM NaCl, and 5 mM imidazole. This was followed by a wash of 20 CVs of of 20 mM Tris, pH 8.0, 500 mM NaCl, and 60 mM imidazole. The purified *Tc*AANAT0 was eluted in 1.0 mL fractions with 20 mM Tris, pH 8.0, 500 mM NaCl, and 500 mM imidazole. The protein concentration in each fraction was measured using the Bradford assay indexed against BSA as a standard and those fractions containing protein were pooled and dialyzed for 16 hours at 4°C against 20 mM Tris pH 7.9, 200 mM NaCl. Following dialysis, the sample was assayed again for concentration and the purity was assessed via SDS-PAGE gel. Purity was determined to be ≥95% continuously.

Additional purification steps were necessary for crystallization. Following affinity purification, the protein was dialyzed against a buffer of 50 mM Tris HCl, pH 8.0, and 10 mM $CaCl_2$ in preparation for thrombin cleavage of the His_6-tag. Protein (10 mg) was incubated with thrombin agarose resin at 4°C for 24 hours following the recommended procedure. The sample was then loaded onto a Ni-NTA column and the cleaved protein eluted in 1 mL fractions with 20 mM Tris, pH 8.0, 500 mM NaCl, and 60 mM imidazole. SDS-PAGE was used to check the purity of the eluted protein. The appropriate fractions were combined and concentrated using a Millipore ultrafiltration cell. The concentrated sample was further purified via FPLC using a SuperDex 75 gel filtration column. The running buffer was 20 mM Tris pH 7.4, 50 mM NaCl, 1 mM EDTA, and 1 mM DTT and the final purified protein was concentrated to 16.9 mg/mL.

Product characterization

Mass spectrometry was used to demonstrate that the kinetic activity recorded was due to the formation of the acylamine product, and not simply due to hydrolysis of the acyl-CoAs. The product was first generated by incubating 100 μg of *Tc*AANAT0 with 3.5 mM tryptamine, 0.3 mM acetyl-CoA, and 300 mM Tris, pH 8.0 at 30°C for 10 minutes. The enzyme was filtered out using a Millipore 10 kDa spin column and the remaining solution containing the enzymatic product was diluted 500-fold. 20 μL was injected into a Phenomenex Kinetex 2.6 μm C_{18} 100 Å (50 mm × 2.1 mm) reverse phase column coupled to an Agilent 6540 liquid chromatography/quadrupole time-of-flight mass spectrometry (LC/QTOF-MS) in positive ion mode as described previously by Dempsey *et al.*[1] A commercial standard of *N*-acetyltryptamine was also run following the same method. The retention times and high-resolution mass-to-charge ratios of the enzyme product and the commercial standard were then compared to validate the catalytic product of the enzyme.

The retention times and high-resolution mass-to-charge ratios of the enzyme product and the commercial standard are shown in Table S1 to validate the catalytic product of the enzyme. A no-enzyme control was used to confirm that formation of *N*-acetyltryptamine was not occurring independent of *Tc*AANAT0, to any appreciable extent.

Table S1 TcAANAT0 product characterization. *Assay conditions – 300mM Tris, pH 8.0, 1mM acetyl-CoA, 1mM tryptamine,100 μg TcAANAT0.*

Sample	Retention Time (min)	m/z	Intensity
*Tc*AANAT0 assay	3.445	203.1187	266,055.84
N-Acetyltryptamine standard	3.487	203.1188	4,096,377.28
No-enzyme control	3.433	203.1182	1,498.61

Determination of acetyl-CoA binding constants

Isothermal titration calorimetry (ITC) was used to investigate the interaction between acetyl-CoA and *Tc*AANAT0. Experiments were performed on a VP-ITC calorimeter (GE Healthcare) at 30°C. Following Ni-NTA affinity chromatography purification, as described previously, *Tc*AANAT0 was dialyzed overnight against 20 mM Tris, pH 8.0, 100 mM NaCl, 0.5 mM EDTA and 1 mM tris(2-carboxyethyl)phosphine (TCEP). Enzyme samples were then diluted to 40 μM and acetyl-CoA samples of ~10-fold excess were prepared from the same dialysis buffer. Titrations included an initial 0.2 μl injection and 12 subsequent injections of acetyl-CoA, with a 3 min time interval between injections. The data were fit using Origin 7.0 (OriginLab Corporation) with the point of initial injection excluded and using an on-site binding model.

The considerable enthalpic contribution (ΔH = -9.49 ± 0.13 kcal/mol) and unfavorable entropic contribution ($-T\Delta S$ = 0.639 kcal/mol) indicate that binding of acetyl-CoA significantly stabilizes the structure of *Tc*AANAT0.

Figure S1: ITC measurements of acetyl-CoA binding to TcAANAT0. *Titrations included an initial 0.2 μl injection and 12 subsequent injections of 500 μM acetyl-CoA into 40 μM TcAANAT0, with a 3 min time interval between injections.*

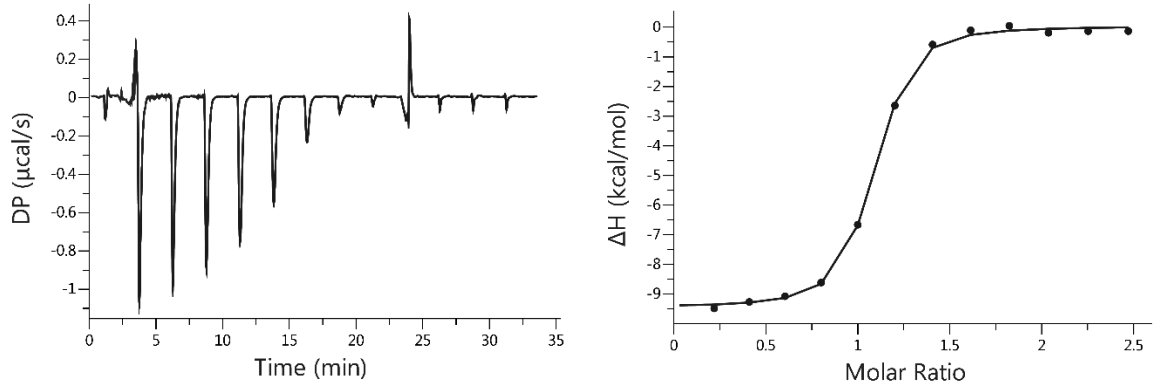

Time Dependent Inhibition

Inhibition plots resulted in competitive and non-competitive apparent K_I values of 25 ± 1.9 μM and 120 ± 3.7 μM against acetyl-CoA and tryptamine respectively (Figure S1). To measure the time-dependence of CoA-S-acetyltryptamine, the rate of reaction was measured at 3 mM tryptamine and 250 μM acetyl-CoA. Enzyme concentration was kept low to ensure the longest possible steady-state duration in the absence of inhibitor. Consecutive measurements were then made at 20, 30, 100 and 200 μM CoA-S-acetyltryptamine (Figure S2A). The resulting progress curves were fit using SigmaPlot 12.0 to Equation S1, where v_i is the initial rate, and v_f is the final rate in order to calculate k_{obs}, the observed first-order rate constant. The rate constant of dissociation, k_{off}, was measured directly via jump dilution. Enzyme at 40 μM was incubated for 10 min. with 250 μM of CoA-S-acetyltryptamine. After incubation, 1 μL of this mixture was then

used to initiate the reaction, resulting in a 750-fold dilution of inhibitor. These data were then fit to Equation S1, with v_i measured as 1.0 μmoles/min and v_f measured as 7.1 μmoles/min (Figure S2B). This allowed k_{on}^{app} to be estimated using Equation S2 under the observation of competitive inhibition against acetyl-CoA binding. A good fit indicated a one-step slow binding mechanism (Figure S2C). The resulting estimate, k_{on}^{app}, was adjusted to account for substrate competition using Equation S3 to give k_{on}^{true}. Finally, the true inhibition constant, K_I^{true} was calculated using Equation S4.

Equation S1

$$[P] = v_f t + \left(\frac{(v_i - v_f)}{k_{obs}}\right)(1 - e^{-k_{obs}t})$$

Equation S2

$$k_{obs} = {k_{on}}^{app}[I] + k_{off}$$

Equation S3

$${k_{on}}^{true} = {k_{on}}^{app}\left(1 + \frac{[S]}{K_M}\right)$$

Equation S4

$${K_I}^{true} = {K_I}^{app}\left(\frac{k_{off}}{{k_{on}}^{true}}\right)$$

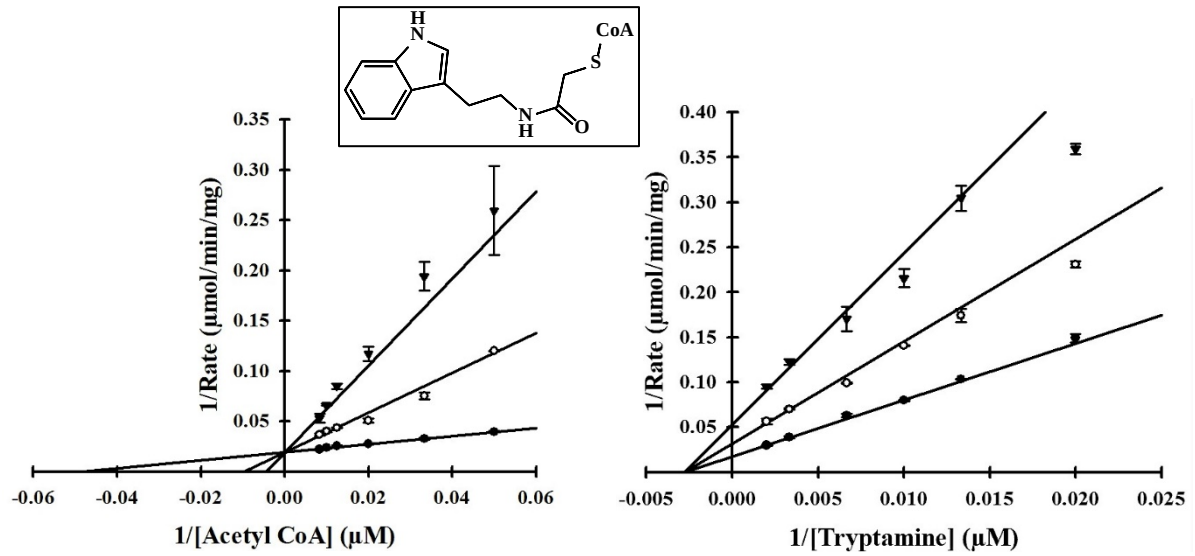

Figure S1: Inhibition plots for CoA-S-acetyltryptamine. *Competitive and non-competitive apparent K_I values of 25 ± 1.9 µM and 120 ± 3.7 µM were measured for acetyl-CoA (left) and tryptamine (right) respectively.*

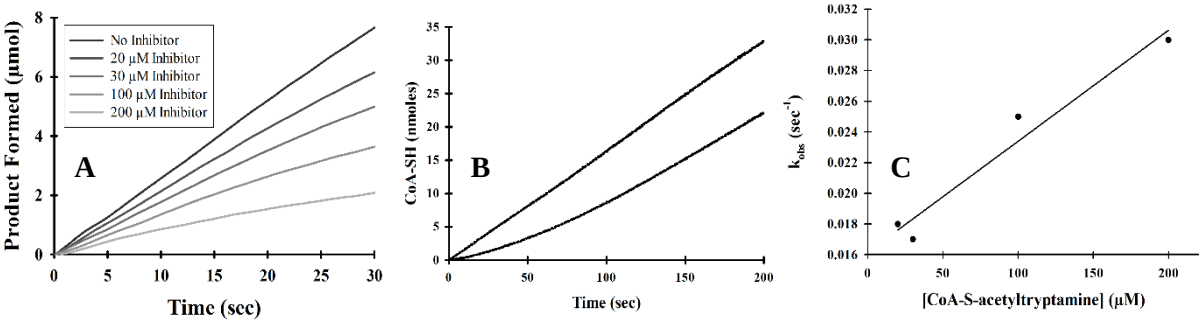

Figure S2 Time-dependent inhibition of TcAANAT0 by CoA-S-acetyltryptamine. *(A) Plot of progress curves of TcAANAT0 saturated with acetyl-CoA and tryptamine and with varying concentrations of inhibitor. (B) Activity regeneration of TcAANAT0 after 10-minute incubation with inhibitor compared against no-incubation control. (C) Plot of k_{obs} vs. [I].*

Table S2: Summary of kinetic rate and inhibition constants attributed to time-dependent inhibition

Kinetic Parameter	
k_5^{app} (M^{-1} s^{-1})	$(7.2 \pm 1.1) \times 10^{1}$
k_5^{true} (M^{-1} s^{-1})	$(7.9 \pm 1.2) \times 10^{2}$
k_6 (s^{-1})	$(1.2 \pm 0.02) \times 10^{-2}$
Half-life (τ) (s)	83 ± 1.2
$K_{i,app,\ acetyl\ CoA}$ (μM)	25 ± 1.9
K_i^{true} (μM)	16 ± 1.7

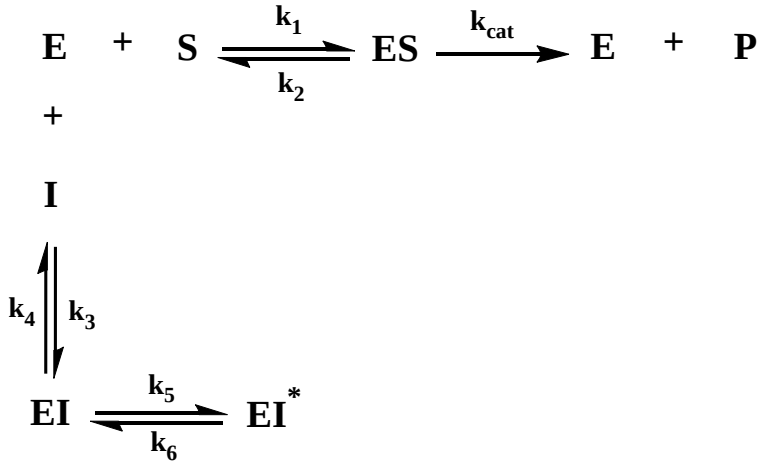

Figure S3: Kinetic model for slow-binding inhibition. *Initial inhibitor binding (k_3) is followed by a second slower step (k_5) induced by a structural reorganization. K_I^{true} is defined by the ratio of k_5 and k_6, the relative formation and relaxation of EI^*, the maximally inhibited complex.*

Insect AANAT Sequence Alignment

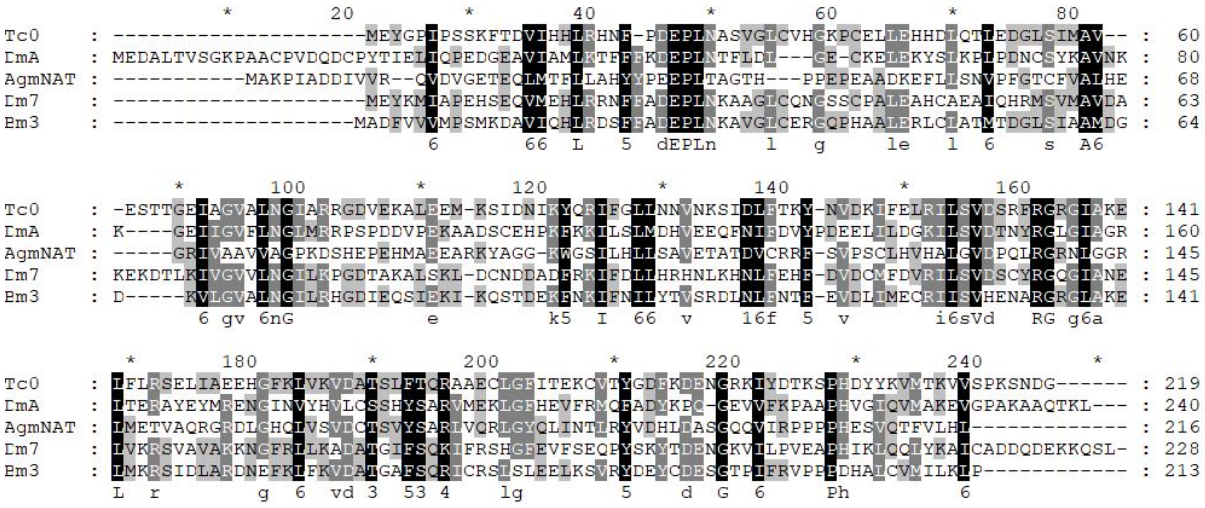

Figure S4: Primary sequence alignment showing conserved Glu residue (within amine binding pocket motif DEPLN) attributed to functioning as a general base in insect AANATs.

Determination of pH-dependence

pH rate profiles were generated to measure the pH-dependence of *Tc*AANAT0 with regards to acetyl CoA binding. Kinetic constants were measured at 0.25 pH increments from pH 5.75 to pH 7.0 and 0.5 pH increments from pH 7.0 to pH 9.5 using the following buffers: MES (pH 5.75 – 6.75), TRIS (pH 7.0 – 8.5) and CHES (pH 9.0 – pH 10.0). Each buffer was made fresh for each individual data set. The data were fit using Visual Enzymics 2010 (IGOR Pro 6.34 A) Equation S5 for a monobasic system with a slope of -2 indicating two unresolvable hydrogen ion dissociation constants, and Equation S6 and Equation S7 for a dibasic system with a acidic leg slope of -1 and -2 respectively. Here, y represents the kinetic constant measured, either K_M, k_{cat}, or k_{cat}/K_M, C represents the maximum value for the kinetic constant, H represents the hydrogen

ion concentration, and K_a, K_1 and K_2 represent the hydrogen ion dissociation constants. All fits were subjected to Levenberg-Marquardt optimization to determine optimal fit.

Equation S5

$$y = \frac{C}{\left(1 + \frac{(K_a)^2}{H^2}\right)}$$

Equation S6

$$y = \frac{C}{\left(1 + \frac{H}{K_1} + \frac{K_2}{H}\right)}$$

Equation S7

$$y = \frac{C}{1 + \frac{H}{K_1} + \frac{K_2}{H} + \frac{K_1 K_2}{H^2}}$$

	Log(k_{cat}) (s^{-1})	Log(k_{cat}/K_M) ($M^{-1}s^{-1}$)
Tryptamine	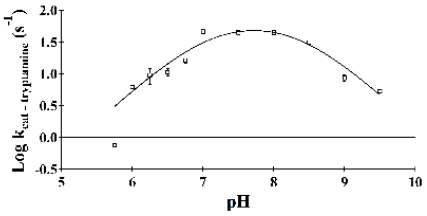	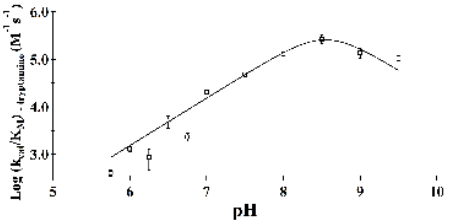
DFPE	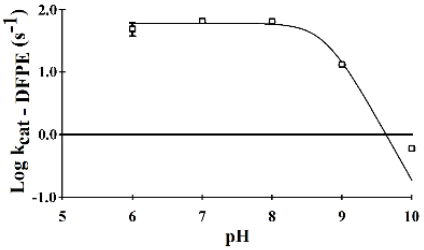	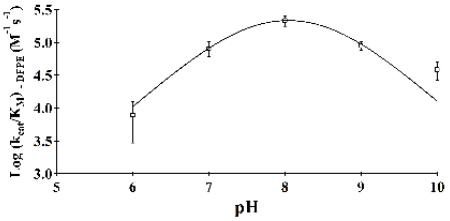
Acetyl-CoA	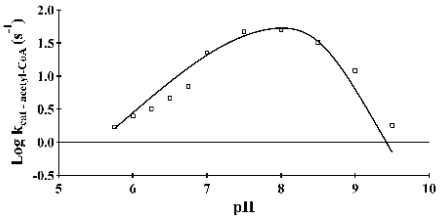	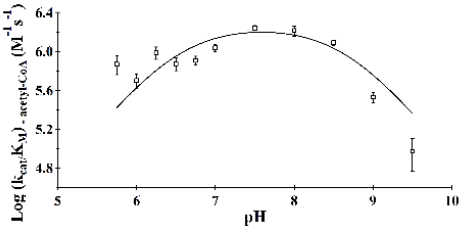

Figure S5 pH rate profiles for tryptamine, DFPE, and acetyl-CoA, illustrating the effect of pH on kcat, and k_{cat}/K_M.

*Tc*AANAT0 Crystallization

Crystal screening was performed using an Art Robbins Instruments Phoenix Liquid Handling robot and several commericially available screens from Qiagen. Hits identified from screening were scaled up. *Tc*AANAT0 was crystallized in 200 mM sodium citrate pH 5.5, and 20% PEG 3000, at 20°C using hanging drops in a 1:1:1 ratio (protein:buffer:acetyl-CoA). Single crystals formed after 3-4 days, and grew to full size in 6-7 days. The crystals were harvested and cryo-cooled using a solution of the crystallization buffer with 20% glycerol and 10 mM acetyl-CoA added.

X-ray Data Collection and Refinement

Data were collected using the 19-BM beamline of the Structural Biology Center (SBC) at the Advanced Photon Source, Argonne, Illinois. Data was processed using iMosflm,[2] and the CCP4 suite was used to refine the data.[3] A homology model for *Tc*AANAT0 was constructed using the structure of *Drosophila melanogaster* arylalkylamine N-acetyltransferase A as a template for molecular replacement.[4] Coot was used to build and refine the complete model.[5] PyMol was used to generate all protein structure figures.[6]

Table S3: X-ray data collection and refinement statistics for TcAANAT0.
****Value denotes highest resolution shell (2.1 Å).***

Data Collection	
Structure (PDB ID)	*Tc*AANAT0 (6V3T)
Space Group	C2
Cell Dimensions	
a, *b*, *c* (Å)	76.14
	131.66
	178.36
α, β, γ (°)	90
	90.05
	90
Resolution (Å)	89.18 – 2.84
Number of Reflections	41256
R_{merge} (%)	7.6
I / *óI*	10.5 (2.1)*
Completeness (%)	100.0
Redundancy	3.8 (3.8)
Refinement	
Resolution (Å)	50 – 2.84
R_{work}/R_{free} (%)	23.5/30.8
Number of Heavy Atoms	
Protein	10219
Ligand/Ion	306
Water	2
B-Factors (Å^2)	
Protein	56.81
Ligand/Ion	62.44
Water	64.84
Ramachandran Plot	
Most Favored Region (%)	88.6
Additionally Allowed (%)	11.3
Generously Allowed (%)	0.1

References

(1) Dempsey, D. R.; Jeffries, K. A.; Anderson, R. L.; Carpenter, A.-M.; Ospina, S. R.; Merkler, D. J. Identification of an Arylalkylamine N-Acyltransferase from Drosophila Melanogaster That Catalyzes the Formation of Long-Chain N-Acylserotonins. *FEBS Lett.* **2014**, *588* (4), 594–599. https://doi.org/10.1016/j.febslet.2013.12.027.

(2) Battye, T. G. G.; Kontogiannis, L.; Johnson, O.; Powell, H. R.; Leslie, A. G. W. iMOSFLM: A New Graphical Interface for Diffraction-Image Processing with MOSFLM. *Acta Crystallogr. D Biol. Crystallogr.* **2011**, *67* (Pt 4), 271–281. https://doi.org/10.1107/S0907444910048675.

(3) Collaborative Computational Project, Number 4. The CCP4 Suite: Programs for Protein Crystallography. *Acta Crystallogr. D Biol. Crystallogr.* **1994**, *50* (Pt 5), 760–763. https://doi.org/10.1107/S0907444994003112.

(4) Dempsey, D. R.; Jeffries, K. A.; Bond, J. D.; Carpenter, A.-M.; Rodriguez-Ospina, S.; Breydo, L.; Caswell, K. K.; Merkler, D. J. Mechanistic and Structural Analysis of Drosophila Melanogaster Arylalkylamine N-Acetyltransferases. *Biochemistry (Mosc.)* **2014**, *53* (49), 7777–7793. https://doi.org/10.1021/bi5006078.

(5) Emsley, P.; Cowtan, K. Coot: Model-Building Tools for Molecular Graphics. *Acta Crystallogr. D Biol. Crystallogr.* **2004**, *60* (Pt 12 Pt 1), 2126–2132. https://doi.org/10.1107/S0907444904019158.

(6) DeLano, W. L. Pymol: An Open-Source Molecular Graphics Tool. *CCP4 Newsl. Protein Crystallogr.* **2002**, *40* (1), 82–92.